Int. J. Electron. Commun. (AEÜ) 143 (2022) 154031

Contents lists available at ScienceDirect

International Journal of Electronics and Communications

journal homepage: www.elsevier.com/locate/aeue

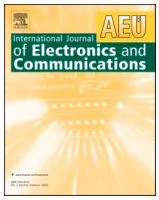

Performance analysis of antenna selection scheme in dual-hop NOMA HD and FD energy harvesting relay networks

Büşra Demirkol [a,*], Mahmoud Aldababsa [b], Mesut Toka [a,c], Oğuz Kucur [a]

[a] Department of Electronics Engineering, Gebze Technical University, Turkey
[b] Department of Electrical and Electronics Engineering, Istanbul Gelisim University, Turkey
[c] Department of Electrical and Computer Engineering, Ajou University, Suwon, South Korea

ARTICLE INFO

Keywords:
Antenna selection
Energy harvesting
Full-duplex
Half-duplex
Non-orthogonal multiple access

ABSTRACT

In this paper, the outage probability (OP) performance of antenna selection schemes is investigated in downlink non-orthogonal multiple access based energy harvesting amplify-and-forward relay network. In this network, base station with multiple antennas simultaneously communicates with multiple-antenna users via the relay, which is equipped with single transmit and multiple receive antennas and operates in half-duplex (HD) or full-duplex (FD) mode. The joint transmit-receive antenna selection and receive antenna selection schemes are employed in the first and second hops, respectively. For the proposed system, the closed-form expressions for the exact OP are derived jointly for HD and FD modes over Nakagami-*m* fading. Then, the corresponding asymptotic OP expressions are obtained. Finally, accuracy of our analyses is verified by simulations.

1. Introduction

In recent years, with the rapid development of wireless communication networks, non-orthogonal multiple access (NOMA) has emerged as a promising multiple access technique to fulfill requirements of fifth-generation (5G) and beyond wireless communication specifications, such as high spectral efficiency and massive connectivity. Different from the currently employed orthogonal multiple access (OMA) techniques, NOMA serves multiple users simultaneously by using the same spectrum resources [1,2]. In the power domain NOMA, simultaneous transmission between the base station (BS) and users is established by using superposition coding at the transmitter and successive interference cancellation (SIC) at the receiver. In this context, users are allocated different power levels depending on their channel gains by the BS, i.e., the stronger users are allocated less power while the weaker users more power. Thus, NOMA can provide a good balance between user fairness and system efficiency, also satisfy massive connectivity and low latency [1–3].

Multiple-input multiple-output (MIMO) techniques, which have benefits such as increasing capacity and improving system performance of wireless communication systems, have been used in NOMA networks to further improve the system performance [4]. In [5], performance of joint antenna selection for MIMO-NOMA networks is investigated under Nakagami-*m* fading channels. In [6], the outage probability (OP) of NOMA with Alamouti space–time block coding scheme, where one BS serves multiple users simultaneously, is analyzed and the authors show that this scheme can double the diversity order of NOMA. Transmit antenna selection (TAS) scheme, which is commonly used in order to reduce system complexity and power consumption, has been applied to multi-user multiple-input single-output (MISO) NOMA network in [7], where higher sum-rate is obtained compared to single antenna case. In [8], antenna selection and user scheduling problems in massive MIMO-NOMA networks have been studied for single-band two-user and multi-band multi-user scenarios, and two algorithms have been proposed to solve these problems. The results show that the efficient search algorithm has achieved optimal performance, and the joint antenna and user selection algorithm has similar performance to the existing methods. In [9], the authors introduce non-regenerative massive MIMO-NOMA relay systems with a multi-antenna source, multi-relay and multi-user. By adopting a maximum mean square error (MMSE)-SIC receiver design, they have derived the closed-form expression of signal-to-interference-plus-noise ratio (SINR) and using this expression, obtained the closed-form expressions of the capacity and sum rate. In [10], antenna selection problem is investigated for a two-user MIMO-NOMA network. Two algorithms have been proposed to maximize the system sum-rate, and it has been observed that both of the proposed algorithms provide

* Corresponding author.
E-mail address: busrademirkol@gtu.edu.tr (B. Demirkol).

https://doi.org/10.1016/j.aeue.2021.154031
Received 12 July 2021; Accepted 5 November 2021
Available online 11 November 2021

significant performance gains. The proposed algorithms in [10] have been developed for NOMA with fixed power allocation and cognitive radio-inspired power allocation scenarios. In [11], the OP of single-hop downlink MIMO-NOMA network, which has one BS with two antennas and multiple users with multiple antennas, has been investigated. In this study, two new antenna selection techniques are proposed based on the decision of the majority of users; majority-based TAS/maximum ratio combining (TAS-*maj*/MRC) and joint transmit and receive antenna selection (JTRAS-*maj*). The closed form expression of the OP for the proposed majority-based schemes has been obtained in the presence and absence of channel estimation errors (CEEs) and feedback delay (FBD). In [12], the closed form expression of exact bit error rate of the JTRAS-*maj* technique in NOMA networks is derived for binary phase shift keying modulation over Nakagami-*m* fading channels in the presence of CEE, FBD and imperfect SIC.

To combine NOMA with relay networks which have the ability of expanding coverage area, increasing system capacity and transmission data rate has attracted interests of many researchers [13]. In dual-hop relaying networks, several relay protocols are proposed, however commonly used ones are amplify-and-forward (AF) and decode-and-forward (DF) [14]. In AF protocol, the relay amplifies the signal received from the source and transmits it to the destination, while the relay decodes the signal received from the source and transmits it to the destination by re-encoding in the DF protocol. The amplifying factors used for signal transmission in the AF protocol can be classified into mainly two types, channel state information (CSI) based [15] depending on instantaneous CSI in the first hop and fixed gain [16] depending on the average of signal-to-noise ratio (SNR) of the first hop. Also, there are two main relaying techniques called half-duplex (HD) and full duplex (FD) according to the transmission process. In HD relaying technique, the transmission of signal from the source to the destination is carried out in two time intervals. On the other hand, in FD relaying, the relay performs the signal reception and transmission by using the same frequency band in the same time interval [17]. Taking advantages of relaying, the OP of TAS/MRC scheme is examined in NOMA HD relay networks for Rayleigh fading channels in [18]. Subsequently, the authors of [19,20] have investigated OP of the NOMA network considered in [18] for CSI-based and fixed gain relays, respectively, over Nakagami-*m* fading channels. In [21], antenna selection schemes for dual-hop AF relay networks in MIMO-NOMA are examined for Rayleigh fading channels and the system performance is studied in terms of the OP and ergodic sum rate. In [22], in the cooperative NOMA-based network, the system performance is evaluated for two relay scenarios where the user close to BS helps the far user as acting an HD or FD relay.

Besides spectral efficiency of communication systems can be increased by exploiting NOMA, there is another challenging issue in 5G and beyond communication systems not to be overlooked, namely energy efficiency. In this context, for the sake of increasing the energy efficiency of wireless systems, simultaneous wireless information and power transfer (SWIPT) is the most noticable one among all proposed techniques that have been commonly studied in the last decade. The SWIPT method, which energy is harvested from radio frequency (RF) signals, is an energy harvesting (EH) technique that can work in good and bad weather conditions and provides durable power supply [23,24]. Practical receiver architectures of EH devices, namely power splitting relay (PSR) and time switching relay (TSR), that can detect energy and information signals have been evaluated in [25]. Also, in [26–28], TSR and PSR architectures are examined for different wireless systems. In [29], the achievable throughput, symbol error rate and OP analyses are obtained in DF-FD adaptive TSR network over Rician fading channel. The authors in [30] investigated the performance of the non-linear EH-based PSR system using FD relay for both the AF and DF modes. In [31], SWIPT is combined with such cooperative NOMA network, where users close to the source are used as EH relays for far users. Three user selection schemes have been proposed, and the OP and system throughput have been analyzed to characterize the performance of these schemes. In [32], the EH-FD-NOMA system, in which both the source and the relay harvest energy from the power beacon with the TSR protocol, is examined and the closed form OP expression is obtained over Rayleigh fading channels. In [33], three TAS schemes have been investigated in EH multi-antenna DF relay networks over Rayleigh fading channels. The exact analytical expressions of OPs are derived to interpret the impact of feedback delay on the performance. In [34], by using TAS at the BS, MRC at the users and single antenna relay, the OP of TAS/MRC is examined in NOMA-EH relaying networks over Nakagami-*m* fading channels. MIMO-NOMA system, in which BS employs maximal-ratio transmission (MRT) and TAS techiques and determines the best EH relay with single antenna while users adopt MRC technique, has been examined in the presence of imperfect SIC and the OP expression has been obtained over Rayleigh fading channels in [35]. In [36], the NOMA network with FD EH relay, where the near user acts as a relay for the far user, is investigated and the OP expression is obtained over Nakagami-*m* fading channels. The authors of [37] obtained the closed form OP expression of FD NOMA-EH network with single antenna at all nodes. Unlike [36] in [37], there is no direct link between BS and far user and the relay uses time switching protocol. The authors of [38] derived the closed-form expression for the OP in EH-FD cooperative NOMA system, in which relay assists the far user and the near user has direct connection with BS. They have shown that cooperative NOMA with EH improves the OP performance dramatically. In [39], the OP of NOMA-EH relaying system with multiple antennas at all nodes is examined over Nakagami-*m* fading channel for only HD relay. In the investigated system the optimal JTRAS and suboptimal JTRAS-maj schemes are utilized in the first and second hops, respectively.

Motivated by the aforementioned studies, in this paper, we focus on the investigation of optimal JTRAS/receive antenna selection (RAS) schemes in both HD and FD EH relaying based NOMA networks. We consider to use RAS scheme in the second hop since it reduces hardware complexity and power consumption when compared to other diversity techniques. In particular, the exact OP expression is jointly derived over Nakagami-*m* fading channel for the two relaying modes. Then, the upper bound for the OP is derived to achieve diversity order and array gain of the considered network. Finally, we have verified the analytical results by Monte Carlo simulations.

2. System model

The dual-hop MIMO-NOMA relay network, which is considered to consist of a CSI-based AF relay that assists multiple users and operates in HD or FD mode, is given in Fig. 1. The network consists of a *BS* (*S*) with T transmit antennas, L users with R_2 receive antennas and one relay (R) with R_1 receive and single transmit antennas. We assume that direct link does not exist between the BS and mobile users due to poor channel conditions, therefore the transmission from the BS to all users is accomplished only via the relay. The system is designed in accordance with the homogeneous network topology, where all users are clustered relatively close. The channels from the BS to the relay and from the relay to users are assumed to be independent and identically distributed (*i.i.d.*) slow Nakagami-*m* fading with average powers of Ω_{SR} and $\Omega_{RU_l}, l = 1,\ldots,$ L, respectively, and self-interference (SI) at the relay is assumed to be non-fading for the FD mode. In the network, optimal JTRAS and RAS techniques are adopted in the first and second hops, respectively. In particular, the best transmit-receive antenna pair, which provides the highest channel gain, is selected in the first hop. On the other hand,in the second hop, the antenna selection cannot be performed in the same way as the first hop, because selecting the best transmit-receive antenna pair providing the highest channel gain between the relay and users cannot be possible in all channel realizations, even such a case could exist it would require high computational complexity and not be mathematically tractable, either [11]. For simplicity, in the second hop, we assume that the best receive antenna of each user providing the highest channel gain belonging to R-U_l links is selected by the relay. We assume that the

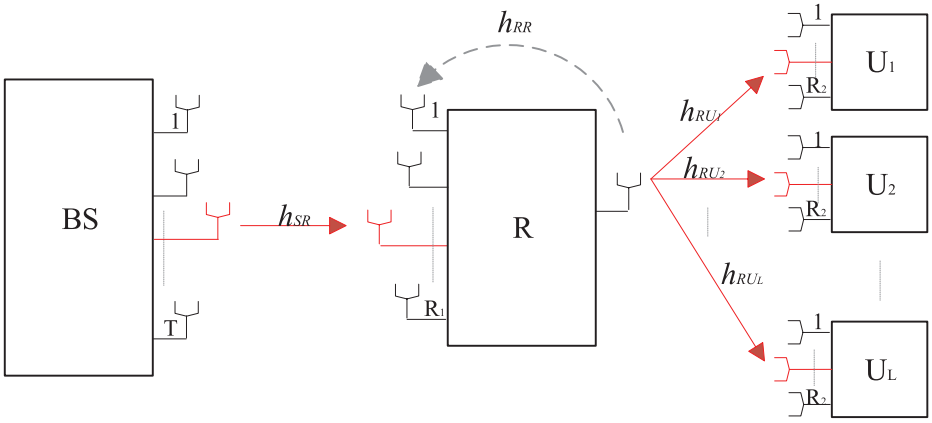

Fig. 1. System model.

perfect CSI and order of the channel gains between the relay and users are available at the BS. In training period, by assuming that links between the relay and mobile users are reciprocal, pilot symbols are sent to the relay by each mobile user in turn such that the best link between the relay and each mobile user is determined at the relay. Then, the BS also sends pilot symbols to the relay such that the best link between the BS and relay is determined at the relay. Afterwards, the relay sends the antenna indices providing the best link to the BS and mobile users. In addition, the order of channel gains for the selected links for the second hop is sent to the BS for power allocation.

In the first hop, the BS transmits the superposed signal $s = \sum_{j=1}^{L} \sqrt{a_j P_S} x_j$ to the relay. Here x_j represents the information symbol with unit energy for user j (U_j), P_S denotes the transmit power of the BS and a_j is the power allocation coefficient subjected to $\sum_{j=1}^{L} a_j = 1$. The received signal at relay is

$$y_R = h_{SR} s + \varpi h_{RR} s_R + n_R, \tag{1}$$

where h_{SR} is Nakagami-m fading channel coefficient of the best transmit-receive antenna pair in the first hop, and n_R is complex additive Gaussian noise (AGN). ϖ denotes HD or FD mode; such that $\varpi = 1$ and $\varpi = 0$ represents FD and HD mode, respectively. Here, h_{RR} is the SI channel coefficient between the transmit and selected receive antenna of the relay. Also, $s_R = G\tilde{y}_R$ is the transmitted signal from the relay with power P_R, where G is the amplifying factor. Depending on PSR protocol, we can split the received signal power at the relay into $\beta : 1-\beta$ proportion, one for EH and the other for information proccessing, where β $(0 < \beta < 1)$ denotes the power splitting ratio. The harvested power at relay is given by $P_R = \eta\beta |h_{SR}|^2 P_S$ and $P_R = \frac{\eta\beta |h_{SR}|^2 P_S}{1-\eta\beta |h_{RR}|^2}$ for HD and FD modes, respectively. Here, η $(0 \leqslant \eta \leq 1)$ is the energy conversion efficiency. We assume that $P_R \simeq \eta\beta |h_{SR}|^2 P_S$ for FD mode since $\eta\beta |h_{RR}|^2 \ll 1$.

Then, information part of the received signal at the relay is expressed as

$$\tilde{y}_R = \sqrt{1-\beta} h_{SR} s + \sqrt{1-\beta}\varpi h_{RR} s_R + \tilde{n}_R, \tag{2}$$

where $\tilde{n}_R = \sqrt{1-\beta} n_R$ is complex AGN with zero mean and variance of σ_R^2 at relay, i.e., $\tilde{n}_R \sim CN(0, \sigma_R^2)$. The amplifying factor at the AF relay can be expressed as

$$G = \sqrt{\frac{P_R}{\left(1-\beta\right)|h_{SR}|^2 P_S + \varpi^2 \left(1-\beta\right)|h_{RR}|^2 P_R + \sigma_R^2}} \simeq \sqrt{\frac{\eta\beta}{1-\beta}}. \tag{3}$$

Then the received signal by U_l can be obtained as

$$y_{RU_l} = \sqrt{1-\beta} G h_{SR} h_{RU_l} s + \varpi\sqrt{1-\beta} G h_{RR} h_{RU_l} s_R + G h_{RU_l} \tilde{n}_R + n_{RU_l}, \tag{4}$$

where n_{RU_l} is complex AGN with zero mean and variance of $\sigma_{RU_l}^2$ at U_l, i. e., $n_{RU_l} \sim CN(0, \sigma_{RU_l}^2)$. h_{RU_l} is channel gain of the selected link between the relay node and U_l. Without loss of generality, we assume that $|h_{RU_1}|^2 \leqslant |h_{RU_2}|^2 \leqslant \ldots \leqslant |h_{RU_L}|^2$ and thus $a_1 > a_2 > \ldots > a_L$.

3. Performance analyses

In this section, firstly the end-to-end SINR of the considered relaying network is derived and its statistical properties is examined. Then, the exact and asymptotic OPs are obtained by using the derived SINR expression. We assume that $\sigma_R^2 = \epsilon\sigma_{RU_l}^2 = \sigma^2$ and $\overline{\gamma} = \frac{P_S}{\sigma^2}$ is the average SNR of each link, where ϵ is any constant that expresses the mathematical relation between σ_R^2 and $\sigma_{RU_l}^2$.

3.1. Statistical properties

In both hops, all the channel coefficients are modeled as *i.i.d.* Nakagami-m distributed random variables. A transmit-receive antenna pair in the first hop and a receive antenna at each user are selected by the maximum squared absolute magnitude. Then, the channel gains related to selected links between S-R and R-U_l are expressed respectively as

$$|h_{SR}|^2 = max_{1 \leqslant i \leqslant T, 1 \leqslant j \leqslant R_1} \left\{ |h_{i,j}|^2 \right\}, \tag{5}$$

$$|\tilde{h}_{RU_l}|^2 = max_{1 \leqslant k \leqslant R_2} \left\{ |h_k^l|^2 \right\}, l = 1, 2, .., L \tag{6}$$

where $h_{i,j}$ denotes the channel coefficient between the ith transmit antenna of the BS and the jth receive antenna of the relay. Also, h_k^l is the channel coefficient between the transmit antenna of the relay and the kth receive antenna of the U_l. According to [40], and by using binomial expansion in [41, eq.(1.111)], the cumulative distribution functions (CDFs) of h_{SR} and non-ordered $\tilde{h}_{RU_l}$ are respectively given as

$$F_{|h_{SR}|^2}\left(x\right) = \left[1 - e^{-\frac{xm_{SR}}{\Omega_{SR}}} \sum_{s=0}^{m_{SR}-1} \left(\frac{xm_{SR}}{\Omega_{SR}}\right)^s \frac{1}{s!}\right]^{TR_1}, \tag{7}$$

$$F_{|\tilde{h}_{RU_l}|^2}\left(x\right) = \left[1 - e^{-\frac{xm_{RU}}{\Omega_{RU_l}}} \sum_{q=0}^{m_{RU}-1} \left(\frac{xm_{RU}}{\Omega_{RU_l}}\right)^q \frac{1}{q!}\right]^{R_2}, \tag{8}$$

where $\Omega_{SR} = E[|h_{SR}|^2] = d_{SR}^{-\alpha}$, $\Omega_{RU_l} = E[|\tilde{h}_{RU_l}|^2] = \Omega_{RU} = d_{RU}^{-\alpha}$. $E[.]$ denotes the expectation operator, $d_{SR}, d_{RU_l} = d_{RU}$ denote the distances of the first and second hops, respectively, α is the path loss exponent.

Moreover, the probability density funtions (PDFs) of h_{SR} and $\widetilde{h}_{RU_l}$ are respectively obtained as

$$f_{|h_{SR}|^2}\left(x\right) = \frac{TR_1\left(\frac{m_{SR}}{\Omega_{SR}}\right)^{m_{SR}}}{\Gamma[m_{SR}]}\sum_{r=0}^{TR_1-1}\sum_{s=0}^{r(m_{SR}-1)} C_{TR_1-1}^{r}(-1)^r x^{s+m_{SR}-1}e^{-\frac{m_{SR}x(r+1)}{\Omega_{SR}}}\mu_s\left(r, m_{SR}\right), \tag{9}$$

$$f_{\widetilde{|h_{RU_l}|^2}}\left(x\right) = \frac{R_2\left(\frac{m_{RU}}{\Omega_{RU}}\right)^{m_{RU}}}{\Gamma[m_{RU}]}\sum_{p=0}^{R_2-1}\sum_{q=0}^{p(m_{RU}-1)} C_{R_2-1}^{p}(-1)^p x^{q+m_{RU}-1}e^{-\frac{m_{RU}x(p+1)}{\Omega_{RU}}}\mu_q\left(p, m_{RU}\right). \tag{10}$$

Here, $C_B^b = \binom{B}{b}$ and $\mu_n(t, m_X)$ denotes the multinomial coefficients and can be expressed as $\mu_n\left(t, m_X\right) = \frac{1}{n\alpha_0}\sum_{\tau=1}^{n}(t\tau - n + \tau)\alpha_\tau\mu_{n-t}(t, m_X)$ for $n \geqslant 1$ [41, eq.(0.314)], where $\alpha_\tau = (m_X/\Omega_X)^\tau/\tau!, \mu_0(t, m_X) = 1$ and if $\tau > 2m_X - 1$, then $\mu_n(t, m_X) = 0$. In addition, the CDF and PDF of the ordered random variable $|h_{RU_l}|^2$ can be respectively represented as [42]

$$F_{|h_{RU_l}|^2}\left(x\right) = Q_l\sum_{k=0}^{L-l} C_{L-l}^{k}\frac{(-1)^k}{l+k}\left[F_{\widetilde{|h_{RU_l}|^2}}\left(x\right)\right]^{l+k}, \tag{11}$$

$$f_{|h_{RU_l}|^2}\left(x\right) = Q_l\sum_{k=0}^{L-l} C_{L-l}^{k}(-1)^k f_{\widetilde{|h_{RU_l}|^2}}\left(x\right)\left[F_{\widetilde{|h_{RU_l}|^2}}\left(x\right)\right]^{l+k-1}, \tag{12}$$

where $Q_l = L!/(L-l)!(l-1)!$. Hereafter, we use X, Y_l and Z to represent $|h_{SR}|^2$, $|h_{RU_l}|^2$ and $|h_{RR}|^2$, respectively.

3.2. Signal-to-interference-plus-noise ratio (SINR)

Given the concept of NOMA, the stronger (near) user U_l first decodes the information signal of the weaker (far) user U_j since $a_1 > a_2 > \ldots > a_L$. Then, the U_l can decode its own signal by using SIC technique. Therefore, the instantaneous SINR at U_l to detect U_j's information ($j < l$) can be written as

$$\gamma_{j\to l} = \frac{a_j\overline{\gamma}XY_l}{\widetilde{a}_j\overline{\gamma}XY_l + \varpi\eta\beta\overline{\gamma}XZY_l + c_1Y_l + c_2}, \tag{13}$$

where $\widetilde{a}_j = \sum_{k=j+1}^{L} a_k, c_1 = \frac{1}{1-\beta}$ and $c_2 = \frac{1}{\epsilon\eta\beta}$. Then, the SINR for the U_l to detect its own signal can be written as

$$\gamma_l = \frac{a_l\overline{\gamma}XY_l}{\widetilde{a}_l\overline{\gamma}XY_l + \varpi\eta\beta\overline{\gamma}XZY_l + c_1Y_l + c_2}. \tag{14}$$

Also, the SINR for U_L can be expressed as

$$\gamma_L = \frac{a_L\overline{\gamma}XY_L}{\varpi\eta\beta\overline{\gamma}XZY_L + c_1Y_L + c_2}. \tag{15}$$

3.3. Outage probability analysis

In this subsection, we derive the exact OP for each user. To make analysis easier, we assume that the target threshold SINRs are $\gamma_{th_j}^t = \gamma_{th}^t$, where $t \in \{FD, HD\}$ for FD and HD mode, respectively. The OP of the U_l can be obtained as

$$P_{out}^l = 1 - P_r\left(\Lambda_{l,1}, \Lambda_{l,2}, \ldots, \Lambda_{l,l}\right), \tag{16}$$

where $\Lambda_{l,j}$ denotes that the lth user decodes the jth user's information successfully and can be expressed as

$$\Lambda_{l,j} = \left\{\frac{a_j\overline{\gamma}XY_l}{\widetilde{a}_j\overline{\gamma}XY_l + \varpi\eta\beta\overline{\gamma}XZY_l + c_1Y_l + c_2} > \gamma_{th}^t\right\}. \tag{17}$$

Accordingly, by denoting $\phi_l^* = max_{1\leqslant j\leqslant l}[\phi_1, \phi_2, \ldots, \phi_l]$ with $\phi_j = \frac{c_1\gamma_{th}^t}{\overline{\gamma}(a_j - \widetilde{a}_j\gamma_{th}^t - \varpi\eta\beta Z\gamma_{th}^t)}$, the OP of the l^{th} user can be given by

$$\begin{aligned} P_{out}^l &= 1 - P_r\left(Y_l > \frac{c\phi_l^*}{X - \phi_l^*}, X > \phi_l^*\right) \\ &= \underbrace{\int_0^{\phi_l^*} f_X\left(x\right)dx}_{I_1} + \underbrace{\int_{\phi_l^*}^{\infty} F_{Y_l}\left(y_l\right)f_X\left(x\right)dx}_{I_2}, \end{aligned} \tag{18}$$

where, $y_l = \frac{c\phi_l^*}{X - \phi_l^*}$ and $c = \frac{c_2}{c_1}$. Then, by using (11), I_2 in (18) can be reformed as

$$\begin{aligned} I_2 &= \int_{\phi_l^*}^{\infty}\left(1 + Q_l\sum_{k=0}^{L-l}\sum_{p=1}^{R_2(k+l)}\sum_{q=0}^{p(m_{RU}-1)} C_{L-l}^{k}C_{R_2(k+l)}^{p}\frac{(-1)^{k+p}}{l+k}y_l^q e^{-\frac{m_{RU}y_lp}{\Omega_{RU}}}\mu_q\left(p, m_{RU}\right)\right)f_X\left(x\right)dx \\ &= 1 - I_1 + Q_l\sum_{k=0}^{L-l}\sum_{p=1}^{R_2(k+l)}\sum_{q=0}^{p(m_{RU}-1)} C_{L-l}^{k}C_{R_2(k+l)}^{p}\frac{(-1)^{k+p}}{l+k}\mu_q\left(p, m_{RU}\right) \times \underbrace{\int_{\phi_l^*}^{\infty} y_l^q e^{-\frac{m_{RU}y_lp}{\Omega_{RU}}}f_X\left(x\right)dx}_{I_3}. \end{aligned} \tag{19}$$

Now, by using (9), I_3 in (19) can be written as

$$\begin{aligned} I_3 &= \frac{TR_1\left(\frac{m_{SR}}{\Omega_{SR}}\right)^{m_{SR}}}{\Gamma[m_{SR}]}\sum_{r=0}^{TR_1-1}\sum_{s=0}^{r(m_{SR}-1)} C_{TR_1-1}^{r}(-1)^r\mu_s\left(r, m_{SR}\right) \\ &\times \underbrace{\int_{\phi_l^*}^{\infty}\left(\frac{c\phi_l^*}{x - \phi_l^*}\right)^q x^{s+m_{SR}-1}e^{-\left(\frac{m_{RU}pc\phi_l^*}{\Omega_{RU}\left(x-\phi_l^*\right)} + \frac{m_{SR}(r+1)x}{\Omega_{SR}}\right)}dx}_{I_4}. \end{aligned} \tag{20}$$

By substituting $x - \phi_l^* = u$ into (20), then I_4 can be written as

$$I_4 = \sum_{n=0}^{s+m_{SR}-1} C_{s+m_{SR}-1}^{n} c^q \left(\phi_l^*\right)^{q+s+m_{SR}-n-1} e^{-\frac{m_{SR}\left(r+1\right)\phi_l^*}{\Omega_{SR}}} \underbrace{\int_0^\infty u^{n-q} e^{-\left(\frac{m_{RU}pc\phi_l^*}{\Omega_{RU}u}+\frac{m_{SR}(r+1)u}{\Omega_{SR}}\right)} du}_{I_5}. \tag{21}$$

Next, with the help of [41, eq.(3.471.9)], I_5 in (21) can be obtained as

$$I_5 = 2\left(\frac{m_{RU}pc\phi_l^*\Omega_{SR}}{m_{SR}(r+1)\Omega_{RU}}\right)^{\frac{n-q+1}{2}} K_{n-q+1}\left(2\sqrt{\frac{m_{SR}m_{RU}p\left(r+1\right)c\phi_l^*}{\Omega_{SR}\Omega_{RU}}}\right), \tag{22}$$

where $K_r(.)$ is the first order modified Bessel function of the second kind which is available in well-known software programs such as MATHEMATICA and MAPLE. By substituting I_2 into (18), closed-form expression of P_{out}^l is obtained as

$$\begin{aligned} P_{out}^l &= 1 + \frac{2TR_1}{\Gamma[m_{SR}]}\left(\frac{m_{SR}}{\Omega_{SR}}\right)^{m_{SR}} Q_l \sum_{k,p,q,r,s,n} C_{L-l}^{k} C_{R_2(k+l)}^{p} C_{TR_1-1}^{r} C_{s+m_{SR}-1}^{n} \frac{(-1)^{k+p}}{l+k} \mu_q\left(p, m_{RU}\right) \\ &\times \mu_s\left(r, m_{SR}\right) c^q \left(\phi_l^*\right)^{q+s+m_{SR}-n-1} e^{-\frac{m_{SR}\left(r+1\right)\phi_l^*}{\Omega_{SR}}} \left(\frac{m_{RU}pc\phi_l^*\Omega_{SR}}{m_{SR}(r+1)\Omega_{RU}}\right)^{\frac{n-q+1}{2}} \\ &\times K_{n-q+1}\left(2\sqrt{\frac{m_{SR}m_{RU}p\left(r+1\right)c\phi_l^*}{\Omega_{SR}\Omega_{RU}}}\right), \end{aligned} \tag{23}$$

where the notation $\sum_{k,p,q,r,s,n}(.) = \sum_{k=0}^{L-l}\sum_{p=1}^{R_2(k+l)}\sum_{q=0}^{p(m_{RU}-1)}\sum_{r=0}^{TR_1-1}\sum_{s=0}^{r(m_{SR}-1)}\sum_{n=0}^{s+m_{SR}-1}(.)$ is used for mathematical tractability.

3.4. Asymptotic analysis

In this subsection, we examine the asymptotic behavior of the obtained OP. Firstly, P_{out}^l can be rewritten as

$$\begin{aligned} P_{out}^l &= 1 - P_r\left(\frac{XY_l}{Y_l + c} > \phi_l^*\right) \\ &\simeq 1 - P_r\left(\frac{XY_l}{X + Y_l} > \phi_l^*\right). \end{aligned} \tag{24}$$

Then, by using $\frac{1}{2}min\left(X,Y\right) \leqslant \frac{XY}{X+Y} \leqslant min(X,Y)$ [43], the upper bound for P_{out}^l can be given by

$$\begin{aligned} P_{out}^{l,UB} &= 1 - P_r\left(min\left(X, Y_l\right) > \phi_l^*\right) \\ &= F_X\left(\phi_l^*\right) + F_{Y_l}\left(\phi_l^*\right) - F_X\left(\phi_l^*\right)F_{Y_l}\left(\phi_l^*\right). \end{aligned} \tag{25}$$

Now, the high SNR approximation approach proposed in [44] is used to obtain asymptotic expression of the OP. Therefore, for $\overline{\gamma}\to\infty$, then $\phi_l^*\to 0$, the asymptotic expressions for $F_X(\phi_l^*)$ and $F_{Y_l}(\phi_l^*)$ are given by

$$F_X^{\infty}\left(\phi_l^*\right) = \frac{1}{\left(\Gamma[m_{SR}+1]\right)^{TR_1}}\left(\frac{m_{SR}\phi_l^*}{\Omega_{SR}}\right)^{m_{SR}TR_1}, \tag{26}$$

$$F_{Y_l}^{\infty}\left(\phi_l^*\right) = C_L^l \frac{1}{\left(\Gamma[m_{RU}+1]\right)^{lR_2}}\left(\frac{m_{RU}\phi_l^*}{\Omega_{RU}}\right)^{m_{RU}lR_2}. \tag{27}$$

Since the value of the term $F_X(\phi_l^*)F_{Y_l}(\phi_l^*)$ in (25) is very small compared to the other terms, we can neglect it and by substituting (26) and (27) into (25), $P_{out}^{l,UB}(x)$ can be written as

$$\begin{aligned} P_{out}^{l,UB} &= \frac{\left(\frac{m\phi_l^*}{\Omega}\right)^{\tau_1}}{\left(\Gamma[m+1]\right)^{\frac{\tau_1}{m}}} + \frac{C_L^l\left(\frac{m\phi_l^*\varepsilon_1}{\Omega\varepsilon_2}\right)^{\tau_2}}{\left(\Gamma\left[\frac{m}{\varepsilon_2}+1\right]\right)^{\frac{\tau_2\varepsilon_2}{m}}} \\ &= \chi\left(\frac{m\phi_l^*}{\Omega}\right)^{\tau}, \end{aligned} \tag{28}$$

where $\tau_1 = m_{SR}TR_1, \tau_2 = m_{RU}lR_2, \tau = min(\tau_1,\tau_2), \Omega = \Omega_{SR} = \varepsilon_1\Omega_{RU}$ and $m = m_{SR} = \varepsilon_2 m_{RU}$. ε_1 and ε_2 are positive constants, and χ is obtained as

$$\chi = \begin{cases} \frac{1}{\left(\Gamma[m+1]\right)^{\frac{\tau}{m}}} + \frac{C_L^l\left(\frac{\varepsilon_1}{\varepsilon_2}\right)^{\tau}}{\left(\Gamma\left[\frac{m}{\varepsilon_2}+1\right]\right)^{\frac{\tau\varepsilon_2}{m}}} & \tau = \tau_1 = \tau_2 \\ \frac{C_L^l\left(\frac{\varepsilon_1}{\varepsilon_2}\right)^{\tau_2}}{\left(\Gamma\left[\frac{m}{\varepsilon_2}+1\right]\right)^{\frac{\tau_2\varepsilon_2}{m}}} & \tau_1 > \tau_2 \\ \frac{1}{\left(\Gamma[m+1]\right)^{\frac{\tau_1}{m}}} & \tau_1 < \tau_2. \end{cases} \tag{29}$$

From (28) and (29), the array gain and diversity order of the U_l can be respectively stated as

$$G_a^l = (\chi)^{1/\tau}\left(\frac{m}{\Omega}\right)\frac{c_1\gamma_{th}^l}{a_j - \widetilde{a}_j\gamma_{th}^l - \varpi\eta\beta Z\gamma_{th}^l}, \tag{30}$$

$$G_d^l = \tau = min\left(\tau_1,\tau_2\right) = min\left(m_{SR}TR_1, m_{RU}lR_2\right), \tag{31}$$

which means that the diversity order of the U_l is limited by the hop with smaller diversity order.

4. Numerical results

In this section, we present some numerical results to demonstrate accuracy of our analyses and to show the OP performance of investigated system over Nakagami-m fading channels. The presented numerical results show that the theoretical analyses are verified by Monte Carlo simulations. In order to be an example, we present results according to $L = 2$ users. The distance between the BS and mobile users is the assumed to be $d = d_{SR} + d_{RU} = 1$ and the path loss exponent is set as $\alpha = 4$. Unless otherwise stated, the power allocation coefficients are set

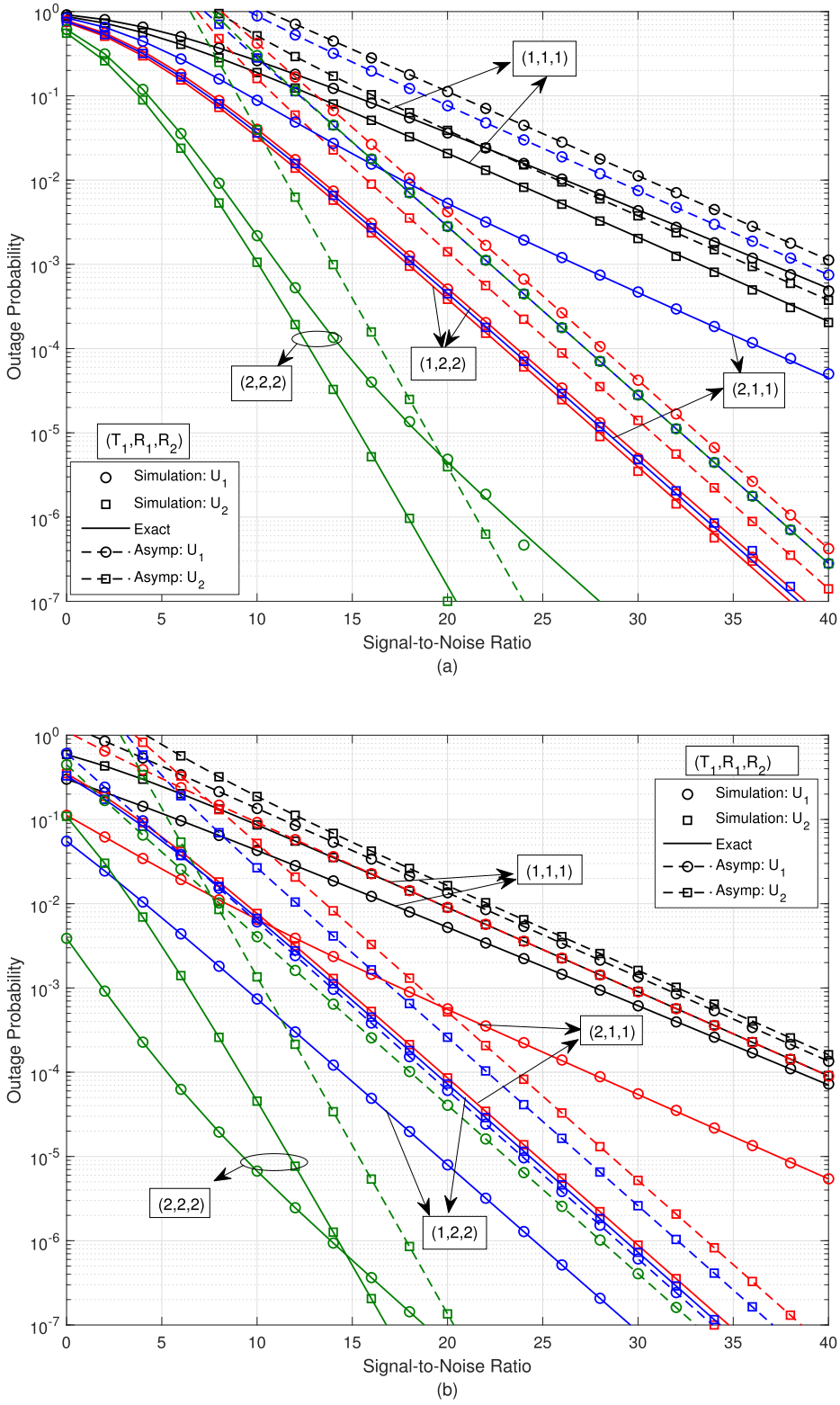

Fig. 2. Outage probability of NOMA-EH scheme in dual hop AF networks versus SNR with varius antenna configurations: (a) HD mode (b) FD mode.

as $a_1 = 0.8$ and $a_2 = 0.2$ which satisfies $a_1 + a_2 = 1$ and the threshold values of users are specified as $\gamma_{th_1}^{HD} = \gamma_{th_2}^{HD} = \gamma_{th}^{HD} = 3$ and $\gamma_{th_1}^{FD} = \gamma_{th_2}^{FD} = \gamma_{th}^{FD} = 1$ respectively, under the condition $a_j > (\widetilde{a}_j + \varpi\eta\beta Z)\gamma_{th}^t$. For conventional JTRAS/RAS-OMA scheme, the threshold values are set as $\gamma_{th} = 3$ and $\gamma_{th} = 15$ for FD and HD modes, respectively, by using the relation of $\frac{1}{2}\sum_{i=1}^{L}\log_2\left(1+\gamma_{th_i}^t\right) = \frac{1}{2}\log_2(1+\gamma_{th})$.

Fig. 2(a) and (b) plot the OP versus the system SNR for different antenna configurations in HD and FD modes, respectively. We set the distances as $d_{SR} = d_{RU} = 0.5$, the Nakagami-m coefficients $m_{SR} = m_{RU} = 1$, the parameters $\eta = 0.9, \beta = 0.5$ and $\epsilon = 0.8$. As clearly seen, the simulation results verify the exact analytical results for each mode and asymptotic curves are accordant with the exact ones. We can see that the increase in the number of antennas improves the system performance

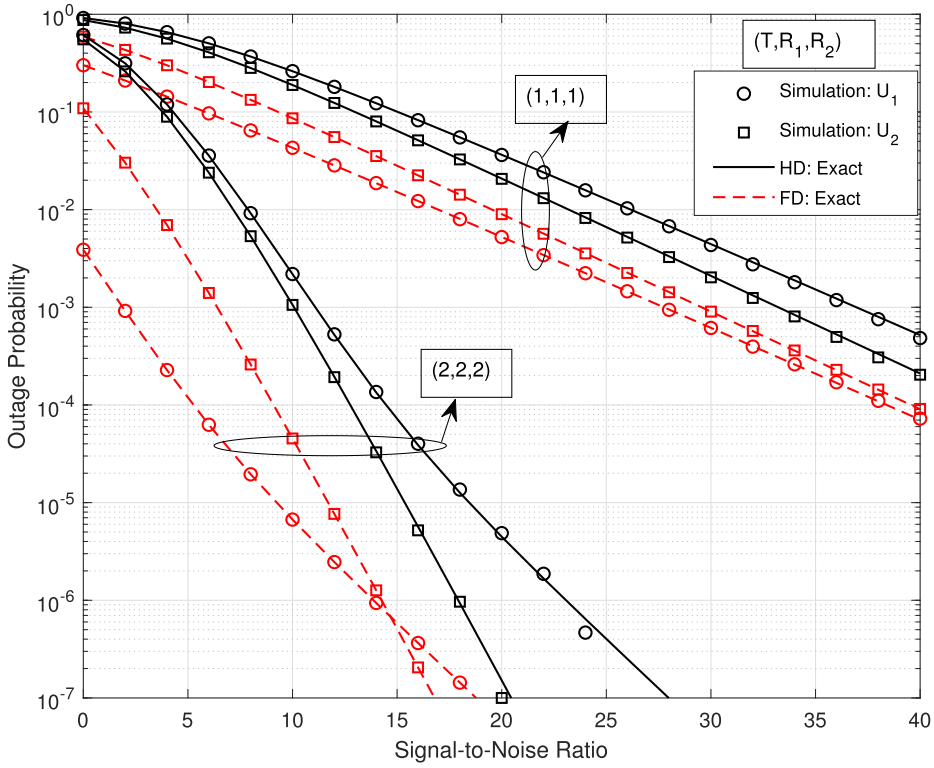

Fig. 3. Comparison of outage probabilities for the FD and the HD modes.

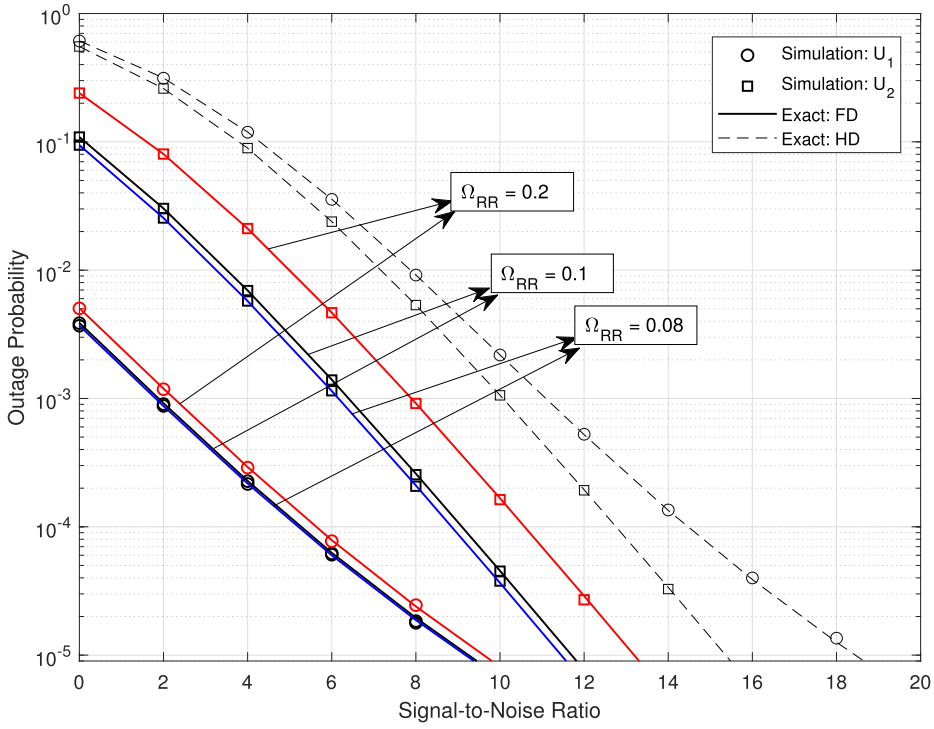

Fig. 4. Comparison of outage probabilities for different Ω_{RR}.

considerably when compared to the scenario without antenna selection. When the number of antennas increases in the first hop, the OP performance of U_2 improves more than that of U_1. On the other hand, the OP performance of both users remarkably enhances as increasing the number of antennas of both hops. In addition, Fig. 2 verifies that the diversity order of the network is $\min(m_{SR}TR_1, m_{RU}lR_2)$. Hence, when $(T, R_1, R_2) = (1,1,1)$, we have $G_d^l = \min(1,l)$, then $G_d^1 = G_d^2 = G_d^3 = 1$. Also, for $(T, R_1, R_2) = (2,2,2)$ we have $G_d^1 = 2, G_d^2 = G_d^3 = 4$. The diversity order of the network, which is limited by the hop with smaller diversity order, can be different for each user.

Fig. 3 demonstrates the OP versus the system SNR for two different antenna configurations for the FD and HD modes. We can see that when the

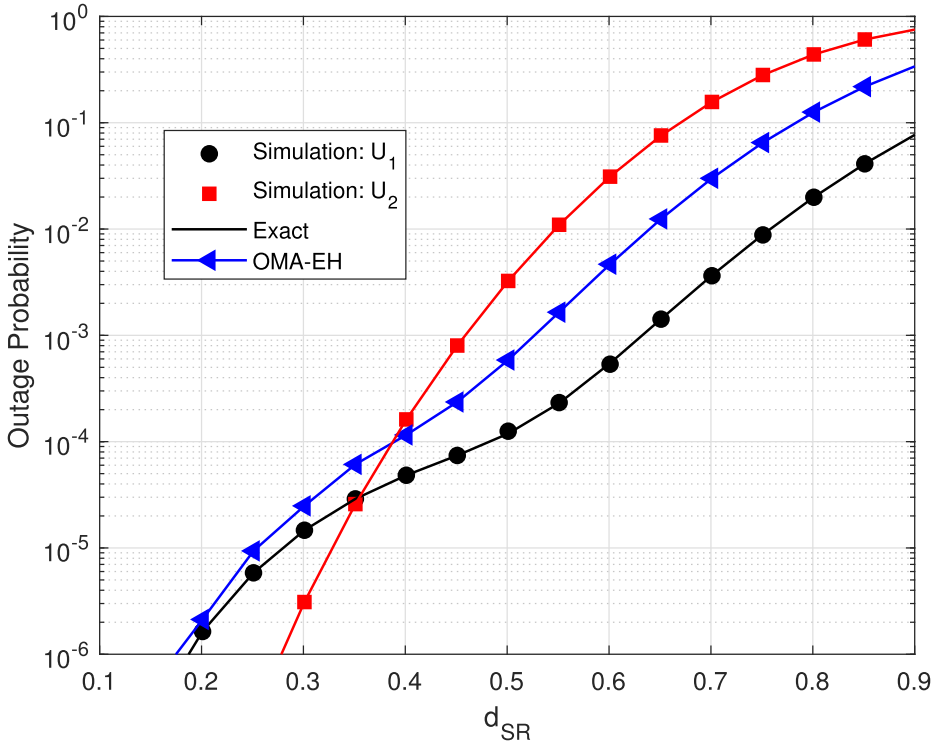

Fig. 5. Outage probability of the system versus d_{SR}.

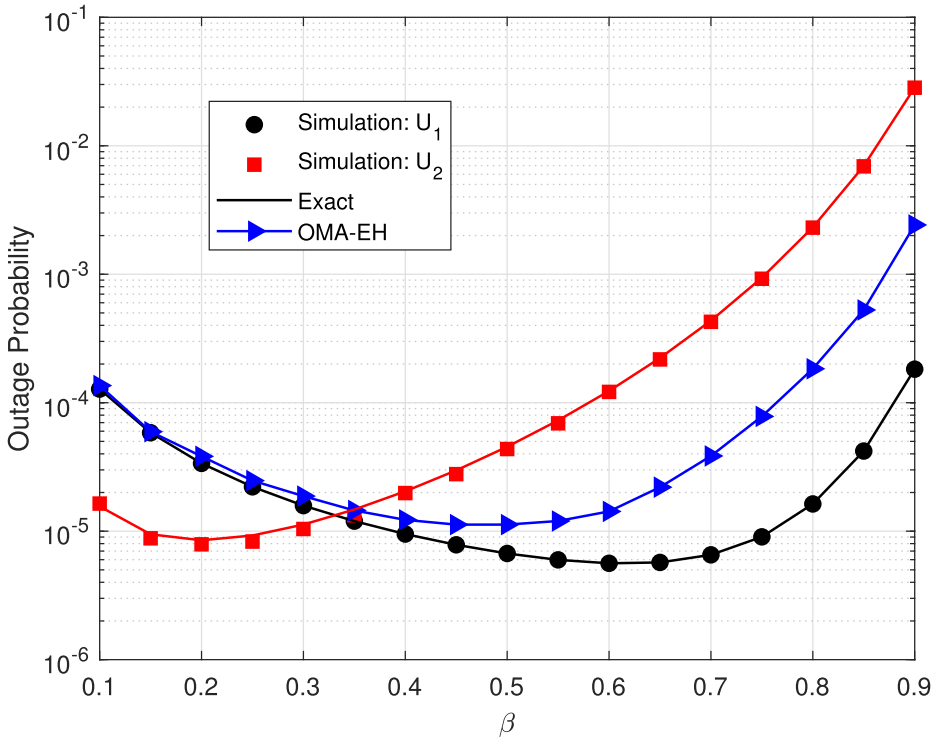

Fig. 6. Outage probability of the system versus β.

relay operates in FD mode, it performs much better than HD mode, for example, for $(T, R_1, R_2) = (2, 2, 2)$ configuration at an OP value of 10^{-6} FD mode provides 9 *dB* and 4 *dB* SNR gains for U_1 and U_2, respectively. When the relay operates in the HD mode, the OP performance of U_2 is better than that of U_1. On the other hand, in the FD mode, while the OP performance of U_1 is better than that of U_2 for the scenario without antenna selection, in antenna configuration of $(T, R_1, R_2) = (2, 2, 2)$ the OP performance of U_1 is better than that of U_2 up to an SNR value of about 15 *dB*, then the situation is reversed. The OP performance of U_1 only depends on the SI from the FD relay, while the performance of U_2 is effected by both the SI of the FD relay and the interference from U_1, and the OP of U_2 can merely suppress the effect of interference after 15 *dB*.

Fig. 4 depicts the effects of the SI at the relay on the performance for different values of Ω_{RR}. The antenna configuration and the Nakagami-m parameters are set as $(T, R_1, R_2) = (2, 2, 2)$ and $m_{SR} = m_{RU} = 1$. As shown in Fig. 4, better performance is obtained for the lower value of Ω_{RR} and the OP performance of U_1 is better than that of U_2 for all Ω_{RR} values. As the value of Ω_{RR} decreases, the SINR at the users increase and then the OP decreases, hence the OP performance is improved. Figs. 5 and 6 plot OP curves of the system versus d_{SR} and β, respectively. In order to obtain the figures, we set $(T, R_1, R_2) = (2, 2, 2)$ and $\overline{\gamma} = 5\ dB$. It is seen that the OP increases as the distance between BS and the relay increases for both users in Fig. 5. One of the reasons for this is that the harvested energy at the relay decreases with the decreasing effect of fading of the channel between the BS and relay. Another reason is the attenuation of the transmitted signal to the users due to the heavy fading effects. In addition, the proposed NOMA scheme outperforms OMA when all d_{SR} values for U_1 and $d_{SR} < 0.39$ for U_2. As can be seen from Fig. 6, the optimum power splitting ratios that provide the best OP for both users are different, since the power allocations of users are different. When the value of β is greater than 0.33, it can be clearly seen that the performance of U_1 is better than that of U_2. It is also observed that the proposed NOMA provides better performance than the conventional OMA, especially for all β values for U_1 and for $\beta < 0.35$ for U_2.

5. Conclusion

In this paper, the performance of JTRAS/RAS scheme in dual-hop AF EH NOMA system is investigated jointly for HD and FD relaying modes over Nakagami-m fading channels. We have obtained the joint closed-form expressions of exact OP and asymptotic OP of the networks for both relaying modes and have verified the analytical results by Monte Carlo simulations. It has been shown that, the performance of the system improves with the increase in the number of antennas when compared to the scenario with no antenna selection. The OP performance of the near user remarkably improves, as the number of antennas increases in the first hop. On the other hand, the OP performances of both users significantly enhance by increasing the number of antennas in both hops. FD mode provides much better performance than HD mode and the performance of the network improves when the power of the SI is lower. Besides, the performance of the network becomes better as the EH relay is closer to the BS and worse as the EH relay closer to the users. In addition, the optimum power splitting ratios for mobile users are different and the far user has larger power splitting ratio. Also, NOMA is better than OMA for all power splitting ratios and distances for the far user while up to some values for the near user. Finally, in cooperative NOMA networks, the performance has been improved by selecting the antennas with the JTRAS/RAS technique and by harvesting energy at the relay.

Declaration of Competing Interest

The authors declare that they have no known competing financial interests or personal relationships that could have appeared to influence the work reported in this paper.

Acknowledgment

This work was supported by the Scientific and Technological Research Council of Turkey (TÜBİTAK) under Grant EEEAG 118E274.

References

[1] Aldababsa M, Toka M, Gökceli S, Kurt GK, Kucur O. A Tutorial on Nonorthogonal Multiple Access for 5G and Beyond. Wireless Commun Mobile Comput 2018;2018:1–24.
[2] Anwar A, Seet B, Li X. Hybrid multiple access for 5G downlink systems: Throughput and outage analysis. AEÜ - Int J Electron Commun 2020;117. article number 153100.
[3] Li QC, Niu H, Papathanassiou AT, Wu G. 5G Network Capacity: Key Elements and Technologies. IEEE Veh Technol Mag 2014;9(1):71–8.
[4] Ding Z, Adachi F, Poor HV. The Application of MIMO to Non-Orthogonal Multiple Access. IEEE Trans Wireless Commun 2016;15(1):537–52.
[5] Li Q, Ge J, Wang Q, Bu Q. Joint antenna selection for MIMO-NOMA networks over Nakagami-m fading channels. In: 2017 IEEE/CIC International Conference on Communications in China (ICCC), Qingdao, China, 2017, p. 1–6.
[6] Toka M, Kucur O. Non-Orthogonal Multiple Access With Alamouti Space-Time Block Coding. IEEE Commun Lett 2018;22(9):1954–7.
[7] Shrestha AP, Han Tao, Bai Zhiquan, Kim JM, Kwak KS. Performance of transmit antenna selection in non-orthogonal multiple access for 5G systems. In: 2016 Eighth International Conference on Ubiquitous and Future Networks (ICUFN), Vienna, Austria, 2016, p. 1031–1034.
[8] Liu X, Wang X. Efficient Antenna Selection and User Scheduling in 5G Massive MIMO-NOMA System. In: 2016 IEEE 83rd Vehicular Technology Conference (VTC Spring), Nanjing, China, 2016, p. 1–5.
[9] Zhang D, Liu Y, Ding Z, Zhou Z, Nallanathan A, Sato T. Performance Analysis of Non-Regenerative Massive-MIMO-NOMA Relay Systems for 5G. IEEE Trans Commun 2017;65(11):4777–90.
[10] Yu Y, Chen H, Li Y, Ding Z, Vucetic B. Antenna selection for MIMO-NOMA networks. In: 2017 IEEE International Conference on Communications (ICC), Paris, France, 2017, p. 1–6.
[11] Aldababsa M, Kucur O. Majority based antenna selection schemes in downlink NOMA network with channel estimation errors and feedback delay. IET Commun 2020;14:2931–43.
[12] Aldababsa M, Kucur O. BER performance of NOMA network with majority based JTRAS scheme in practical impairments. AEÜ-Int J Electron Commun 2021;129. article number 153523.
[13] Ding Z, Peng M, Poor HV. Cooperative Non-Orthogonal Multiple Access in 5G Systems. IEEE Commun Lett 2015;19(8):1462–5.
[14] Laneman JN, Tse DNC, Wornell GW. Cooperative diversity in wireless networks: Efficient protocols and outage behavior. IEEE Trans Inf Theory 2004;50(12):3062–80.
[15] Hasna MO, Alouini M-. End-to-end performance of transmission systems with relays over Rayleigh-fading channels. IEEE Trans Wireless Commun 2003;2(6):1126–31.
[16] Hasna MO, Alouini M-. A performance study of dual-hop transmissions with fixed gain relays. IEEE Trans Wireless Commun 2004;3(6):1963–8.
[17] Zhang Z, Long K, Vasilakos AV, Hanzo L. Full-Duplex Wireless Communications: Challenges, Solutions, and Future Research Directions. Proc IEEE 2016;104(7):1369–409.
[18] Men J, Ge J. Non-Orthogonal Multiple Access for Multiple-Antenna Relaying Networks. IEEE Commun Lett 2015;19(10):1686–9.
[19] Zhang Y, Ge J, Serpedin E. Performance Analysis of Nonorthogonal Multiple Access for Downlink Networks With Antenna Selection Over Nakagami-m Fading Channels. IEEE Trans Veh Technol 2017;66(11):10590–4.
[20] Aldababsa M, Kucur O. Outage performance of NOMA with TAS/MRC in dual hop AF relaying networks. In: 2017 Advances in Wireless and Optical Communications (RTUWO), Riga, Latvia, 2017, p. 137–141.
[21] Aldababsa M, Kucur O.s Cooperative NOMA with Antenna Selection Schemes. In: 2019 27th Signal Processing and Communications Applications Conference (SIU), Sivas, Turkey, 2019, p. 1–4.
[22] Yue X, Liu Y, Kang S, Nallanathan A, Ding Z. Outage performance of full/half-duplex user relaying in NOMA systems. In: 2017 IEEE International Conference on Communications (ICC), Paris, France, 2017, p. 1–6.
[23] Varshney LR. Transporting information and energy simultaneously. In: 2008 IEEE International Symposium on Information Theory, Toronto, ON, Canada, 2008, p. 1612–1616.
[24] Zhou X, Zhang R, Ho CK. Wireless Information and Power Transfer: Architecture Design and Rate-Energy Tradeoff. IEEE Trans Commun 2013;61(11):4754–67.
[25] Nasir AA, Zhou X, Durrani S, Kennedy RA. Relaying Protocols for Wireless Energy Harvesting and Information Processing. IEEE Trans Wireless Commun 2013;12(7):3622–36.
[26] Di X, Xiong K, Fan P, Yang H. Simultaneous Wireless Information and Power Transfer in Cooperative Relay Networks With Rateless Codes. IEEE Trans Veh Technol 2014;66(4):2981–96.
[27] Zhou X, Zhang R, Ho CK. Wireless Information and Power Transfer in Multiuser OFDM Systems. IEEE Trans Wireless Commun 2014;13(4):2282–94.
[28] Zhang R, Ho CK. MIMO Broadcasting for Simultaneous Wireless Information and Power Transfer. IEEE Trans Wireless Commun 2012;12(5):1989–2001.

[29] Nguyen TN, Tran M, Nguyen T-L, Voznak M. Adaptive relaying protocol for decode and forward full-duplex system over Rician fading channel: System performance analysis. China Commun 2019;16(3):92–102.
[30] Tin TP, Van PD, Hung HD, Tan NN, Minh T, Miroslav V. Non-linear energy harvesting based power splitting relaying in full-duplex AF and DF relaying network: system performance analysis. Proc Estonian Acad Sci 2020;12:368–81.
[31] Liu Y, Ding Z, Elkashlan M, Poor HV. Cooperative Non-orthogonal Multiple Access With Simultaneous Wireless Information and Power Transfer. IEEE J Sel Areas Commun 2016;34(4):938–53.
[32] Nguyen BC, Hoang TM, Tran PT, Nyugen TN. Outage Probability of NOMA System with Wireless Power Transfer at Source and Full-duplex Relay. AEÜ - Int J Electron Commun 2020;116. article number 152957.
[33] Huang Y, Wang J, Zhang P, Wu Q. Performance Analysis of Energy Harvesting Multi-Antenna Relay Networks With Different Antenna Selection Schemes. IEEE Access 2017;6:5654–65.
[34] Han W, Ge J, Men J. Performance analysis for NOMA energy harvesting relaying networks with transmit antenna selection and maximal ratio combining over Nakagami-m fading. IET Commun 2016;10:2687–93.
[35] Le TA, Kong HY. Energy harvesting relay-antenna selection in cooperative MIMO/NOMA network over Rayleigh fading. Wireless Netw 2020;26:2075–87.
[36] Wang S, Wang C, Chung W. Exact Performance of NOMA with Full-Duplex Energy Harvesting Relaying in Nakagami-m Frequency-Selective Fading Channel. In: 2018 IEEE Global Conference on Signal and Information Processing (GlobalSIP), Anaheim, CA, USA, 2018, p. 818–822.
[37] Guo C, Zhao L, Feng C, Ding Z, Chen H. Energy Harvesting Enabled NOMA Systems With Full-Duplex Relaying. IEEE Trans Veh Technol 2019;68(7):7179–83.
[38] Deepan N, Rebekka B. Outage Performance of Full duplex Cooperative NOMA with Energy harvesting over Nakagami-m fading channels. In: 2019 TEQIP III Sponsored International Conference on Microwave Integrated Circuits, Photonics and Wireless Networks (IMICPW), Tiruchirappalli, India, 2019, p. 435–439.
[39] Aldababsa M, Basar E. Joint Transmit and Receive Antenna Selection System for MIMO-NOMA with Energy Harvesting, arXiv:2103.15504, 2021.
[40] David H, Nagaraja N. Order Statistics. 3rd ed. Hoboken, NJ, USA: Wiley; 2003.
[41] Gradshteyn IS, Ryzhic IM. Table of Integrals, series, and Products. 6th ed. New York, USA: Academic; 2000.
[42] Men J, Ge J, Zhang C. Performance Analysis of Nonorthogonal Multiple Access for Relaying Networks Over Nakagami-m Fading Channels. IEEE Trans Veh Technol 2017;66(2):1200–8.
[43] Anghel PA, Kaveh M. Exact symbol error probability of a Cooperative network in a Rayleigh-fading environment. IEEE Trans Wireless Commun 2004;3(5):1416–21.
[44] Wang Z, Giannakis GB. A simple and general parameterization quantifying performance in fading channels. IEEE Trans Commun 2003;51(8):1389–98.